Disruption of Cooperation Between Ras and MycN in Human Neuroblastoma Cells Promotes Growth Arrest

Shira Yaari,[1] Jasmine Jacob-Hirsch,[3] Ninette Amariglio,[3] Ronit Haklai,[1] Gideon Rechavi,[2,3] and Yoel Kloog[1]

Abstract

Purpose: Our aim was to examine whether active Ras and MycN cooperation contributes to the malignant phenotype of human neuroblastoma with amplified *MycN* gene, an aggressive incurable tumor.

Experimental Design: Human neuroblastoma LAN-1 cells, in which the *MycN* gene is amplified, were used to examine the impact of the Ras inhibitor farnesylthiosalicylic acid on cell growth, on the levels Ras and MycN proteins, and on profiles of gene expression.

Results: We show that LAN-1 cells express relatively large amounts of MycN and active Ras-GTP. Inhibition of active Ras by farnesylthiosalicylic acid led to attenuation of the Raf-MEK-ERK and phosphoinositide 3-kinase-Akt-glycogen synthase-3 (GSK-3) pathways, to reduction in cyclin D1, phospho-retinoblastoma, and E2F, and to increase in the cyclin-dependent kinase inhibitor p27 and in retinoblastoma-binding protein-1, an inhibitor of E2F transcriptional activity. Ras inhibition by farnesylthiosalicylic acid or by a dominant-negative Ras also led to complete disappearance of MycN protein from the nuclei of LAN-1 cells. This was a result of blocking of Akt inactivation of GSK-3, leading to GSK-3-dependent phosphorylation with consequent proteosomal degradation of MycN. Loss of active Ras and of MycN in LAN-1 cells was manifested in profiles of gene expression that could be expected from the loss of MycN transcriptional activity and of Ras signaling. These changes explain the farnesylthiosalicylic acid – induced inhibition of LAN-1 cell growth.

Conclusions: Active Ras is needed to block MycN degradation, promoting cooperative Ras- and MycN-dependent cell cycle progression in LAN-1 cells. Ras inhibitors are therefore likely candidates for the treatment of advanced neuroblastoma characterized by high expression of MycN.

Cooperation between Ras and Myc is an important paradigm of cellular transformation (1). The Ras proteins act essentially as extracellularly regulated relay systems. They are activated by extracellular signals that promote guanine-nucleotide exchange factor-mediated exchange of GDP for GTP on Ras (2). The active GTP-bound Ras in turn activates a multitude of downstream effectors, including Raf-1, phosphoinositide 3-kinase (PI3K), and Ral-guanine-nucleotide exchange factors, which regulate cell proliferation, differentiation, survival, and death (3). In many human tumors, Ras is chronically active (4). This is largely attributable to activating mutations in *Ras* genes, but also to alterations in upstream components such as receptor tyrosine kinases that activate Ras (5). The chronically active Ras contributes to uncontrolled cell growth and cell death, and—in cooperation with Myc, other oncogenes, and tumor suppressors—leads to malignant transformation.

The Myc proteins are short-lived nuclear transcription factors that regulate cell growth and apoptosis (1). Defects in the Myc and the retinoblastoma/E2F pathways in conjugation with abnormalities in the Ras pathways are common in many human tumors (1, 6, 7). Ras activation facilitates c-Myc functions in cell cycle progression and at the same time blocks the proapoptotic effects of c-Myc (1, 8). c-Myc activity contributes to progression of the G_1-S phase through induction of cyclin D/cyclin-dependent kinase (Cdk)-4 or cyclin E/Cdk2 or both, leading to the phosphorylation and inactivation of retinoblastoma family members and the liberation of E2F (1, 6). Ras signaling also results in the activation of cyclin D/Cdk4 and the retinoblastoma/E2F pathway (1, 9–11). Such activities lead to enhanced cell proliferation. An important characteristic of the cooperation between Ras and c-Myc is conferred by the Ras-regulated stabilization of c-Myc. Active Ras promotes the stabilization and accumulation of newly translated c-Myc through Ras-regulated enzymes that posttranslationally modify the NH_2-terminal region of c-Myc (8).

Authors' Affiliations: [1]Department of Neurobiochemistry, The George S. Wise Faculty of Life Sciences, Tel-Aviv University, [2]Sackler School of Medicine, Tel-Aviv University, Tel Aviv, and [3]Department of Pediatric Hemato-Oncology, Safra Children's Hospital and Cancer Research Center, Sheba Medical Center, Tel Hashomer, Israel

Received 10/8/04; revised 12/21/04; accepted 1/11/05.

Grant support: Israel Cancer Association (Y. Kloog). G. Rechavi is incumbent of the Djerassi Chair in Oncology and Y. Kloog is incumbent of the Jack H. Skirball Chair in Applied Neurobiology.

The costs of publication of this article were defrayed in part by the payment of page charges. This article must therefore be hereby marked *advertisement* in accordance with 18 U.S.C. Section 1734 solely to indicate this fact.

Note: Supplementary data for this article are available at http://eng.sheba.co.il/genomics and at Clinical Cancer Research Online (http://clincancerres.aacrjournals.org/).

Requests for reprints: Yoel Kloog, Department of Neurobiochemistry, The George S. Wise Faculty of Life Sciences, Tel-Aviv University, 69978 Tel Aviv, Israel. Phone: 972-3-640-9699; Fax: 972-3-640-7643; E-mail: kloog@post.tau.ac.il.

The NH_2-terminal box 1 region of all Myc isoforms contains two key phosphorylation sites, Thr^{58} and Ser^{62} (8, 12). Phosphorylation of these two sites has opposing effects on c-Myc stability and is carried out in both cases by kinases controlled by Ras (1, 8). Ser^{62} phosphorylation is catalyzed by extracellular signal-regulated kinase (ERK), and results in c-Myc stabilization. Phosphorylation of Thr^{58} is catalyzed by glycogen synthase-3 (GSK-3) and targets c-Myc to the ubiquitin-proteasome protein degradation pathway. GSK-3 itself is negatively regulated by Akt, which phosphorylates and inactivates it (1). Thus, Ras that promotes activation of Akt leads to inactivation of GSK-3 and elimination of c-Myc degradation (1). This seems to result in accumulation of c-Myc in tumor cells characterized by chronically active Ras protein. More recent studies showed that protein phosphatase 2A dephosphorylates Ser^{62} of c-Myc, whose phosphorylation stabilizes c-Myc, prior to its ubiquitination and degradation (13).

Alterations in Myc that are common in many human tumors include mutation of Thr^{58}, which prevents Myc degradation (8), and *Myc* gene amplification, which leads to Myc overexpression (14, 15). The latter is typical of the most aggressive stage IV neuroblastoma (16). These tumors are characterized by amplified *MycN* genes, some of them having >100 copies (15). The strong association between *MycN* gene amplification and aggressiveness of the disease, taken together with the aforementioned Ras-Myc cooperation, suggests that active Ras might contribute significantly to the malignant phenotype of advanced neuroblastoma. This possibility has not been examined up to now, probably because *Ras* gene mutations are rarely found in neuroblastoma (17). Unlike the well-characterized mechanisms of cooperation between c-Myc and Ras, little is known about MycN-Ras interactions. However, because Ras might be chronically active even in the absence of *Ras* gene mutations, it is not unreasonable to assume that advanced neuroblastoma might exhibit significant amounts of active, GTP-bound Ras that cooperates with MycN. This possibility is supported by the knowledge that highly malignant neuroblastoma is characterized by high expression of the TRKB receptor, known to activate Ras pathways (18), and its ligand brain-derived neurotrophic factor, which acts via autocrine loops to enhance neuroblastoma cell proliferation and survival (19). Here we examined whether the cooperation between Ras and MycN contributes to the malignant phenotype of neuroblastoma. We used the cell line, LAN-1, which was derived from advanced human neuroblastoma and possess amplified *MycN* gene (18).

Materials and Methods

Cell lines and reagents. LAN-1 cells and SHEP cells were grown in RPMI 1640 with 10% FCS. Farnesylthiosalicylic acid was prepared as described in detail previously (20, 21). Hoechst dye 33258 was from Sigma-Aldrich (St. Louis, MO); the enhanced chemiluminescence kit was from Amersham (Arlington Heights, IL); mouse anti-pan-Ras antibodies (Ab-3) and mouse anti-MycN (Ab-1) were from Calbiochem (La Jolla, CA); rabbit anti-ERK1/2 antibodies, rabbit anti-cyclin D1 (M-20), rabbit anti-retinoblastoma (C-15), E2F1 (C-20), and rabbit anti-pMycN (Thr^{58}/Ser^{62}) were from Santa Cruz Biotechnology (Santa Cruz, CA); mouse anti-phospho-ERK and rat anti-tubulin antibodies (AK-15) were from Sigma-Aldrich; rabbit anti-phospho-Akt (Ser^{473}) (4E2) was from Cell Signaling Technology (Beverly, MA) and rabbit anti-Raf-1 (C2), and mouse anti–retinoblastoma-binding protein 1 (RBBP1; clone LY11) were from Upstate Biotechnology (Lake Placid, NY). Peroxidase goat anti-mouse IgG, peroxidase goat anti-rabbit IgG, and peroxidase goat anti-rat IgG were from Jackson ImmunoResearch Laboratories (West Grove, PA); carbobenzoxy-L-leucyl-L-leucinal Z-LLL-CHO (MG132), LY294002, and U0126 were from Calbiochem.

Cell growth under farnesylthiosalicylic acid treatment. Cells were maintained at a constant temperature of 37°C in a humidified atmosphere of 95 air/5% CO_2. They were plated at a density of 10^3 cells per well in 24-well plates and then treated with 50 μmol/L farnesylthiosalicylic acid or the vehicle (0.1% Me_2SO). To determine whether farnesylthiosalicylic acid was toxic to cells, we used Hoechst 33258 (1 μg/mL). Cells were incubated with the reagent for 5 minutes and the stained nuclei were visualized under a fluorescence microscope. Cell growth was estimated by direct counting of cells grown in RPMI 1640/10% FCS. LAN-1 cells (10^3 cells per well in 24-well plates) were incubated for the indicated time period in the presence of 0.1% Me_2SO or 3 to 50 μmol/L farnesylthiosalicylic acid. After incubation, the cells were collected and counted.

Fluorescence* in situ *hybridization. The status of the *MycN* gene was determined by fluorescence *in situ* hybridization using the MycN probe (Vysis, Downers Grove, IL) as described previously (22). The slides were analyzed using an Olympus BH2 fluorescence light microscope equipped with a Plan Apo objective 100×/1.4 oil lens, an appropriate spectral filter (BH2-TFC1 Triple Band filter 4′,6-diamidino-2-phenylindole/FITC/TRITC), and a 100 W mercury arc lamp (22).

Assay of Ras, Ras effectors, and cell cycle regulators. To examine the effect of farnesylthiosalicylic acid on Ras in the cultured cells, we plated LAN-1 cells at a density of 1.5×10^6 cells per 10 cm dish and grew them in RPMI 1640/10% FCS. After 12 hours, farnesylthiosalicylic acid (25 or 50 μmol/L) or the vehicle (0.1% Me_2SO) was added, and 48 hours later, the cells were homogenized in 300 μL homogenization buffer, and subjected to subcellular fractionation into 100,000 × *g* pellet (P_{100}) and supernatant (S_{100}) as described (23). Samples containing 30 μg protein were subjected to SDS-PAGE, followed by immunoblotting with 1:2,500 pan-Ras antibodies and 1:7,500 peroxidase goat anti-mouse IgG, as described (23). Ras protein bands were visualized by enhanced chemiluminescence . Alternatively, cells were lysed in 250 μL lysis buffer (23) and samples containing 50 μg cell lysate protein (ERK, phospho-ERK, E2F1, p27 and tubulin) or 100 μg protein (Akt, phospho-Akt, cyclin D1, retinoblastoma and RBBP1) were used for SDS-PAGE and immunoblotting with anti-ERK (1:2,000), anti-phospho-ERK (1:10,000), anti-Akt (1:1,000), anti-phospho-Akt (1:2,000), anti-cyclin D1 (1:1,000), anti-E2F1 (1:200), anti-p27 (1:1,000), anti-retinoblastoma (1:1,000), anti-RBBP1(1:500) or anti-tubulin (1:500) antibodies. Blots were then exposed to the appropriate secondary peroxidase-coupled IgG (1:5,000), and subjected to enhanced chemiluminescence (23). Protein bands were quantified by densitometry with Image Master VDS-CL (Amersham Pharmacia Biotech, Piscataway, NJ) using TINA 2.0 software (Ray Tests).

Ras-GTP assays. Cells (1.5×10^6) were plated in 10 cm dishes and farnesylthiosalicylic acid (25 or 50 μmol/L) was added 1 day later. The cells were then lysed, 48 hours after the drug treatment, in 0.5 mL of Ras-binding domain lysis buffer (24) containing 0.1 mmol/L orthovanadate. Lysates containing 500 μg protein were analyzed for Ras-GTP by the glutathione S-transferase–Ras-binding domain pull-down assay followed by Western immunoblotting with pan anti-Ras antibodies as described previously (23).

Raf-1 kinase assay. We determined Raf-kinase activity using a Raf-1 immunoprecipitation kinase cascade assay kit (Upstate Biotechnology). LAN-1 cells were plated (1.5×10^6 cells in 10 cm dishes), and the next day, farnesylthiosalicylic acid (25 or 50 μmol/L) was added for 48 hours. The cells were then lysed in 0.5 mL of Raf-1 kinase assay kit lysis buffer. Raf-1 was immunoprecipitated from 1.5 mg lysate and assayed in the coupled kinase assay using myelin basic protein (Sigma) as a substrate and [γ-^{32}P]ATP (3,000 Ci/mmol, DuPont, NEN, Boston, MA) as a phosphate donor, according to the manufacturer's

instructions. The amount of ^{32}P-labeled myelin basic protein thus formed was estimated in a scintillation counter.

PI3K assay. LAN-1 cells were treated with farnesylthiosalicylic acid, as described for the Raf-1 kinase assay. We lysed the cells with 0.5 mL of PI3K lysis buffer, immunoprecipitated the enzyme from 1.5 mg lysate with rabbit anti-PI3K p85 antibodies (Upstate Biotechnology), and assayed its activity with 1 mg/mL phosphatidyl inositol, 10 mmol/L ATP, and 5 μCi [γ-^{32}P] ATP (23). After extracting the lipids with chloroform/methanol, we separated them by TLC. Phospholipid markers were used for identification of the ^{32}P-labeled phosphatidyl inositol-3-phosphate product. The ^{32}P-labeled lipid products were visualized by overnight exposure on an X-ray film and the spots were quantified by TINA analysis (23).

Confocal microscopy. We plated 2×10^5 LAN-1 cells on glass coverslips and then treated them with 50 μmol/L farnesylthiosalicylic acid or the vehicle (0.1% Me_2SO). Alternatively, the cells were cotransfected with plasmid DNA coding for Ras17N (1.4 μg) or with a vector control (PCDNA3; 1.4 μg) along with plasmid DNAs coding for green fluorescent protein (GFP; 0.6 μg). The cells were fixed after 48 hours, or after 0, 6, 12, 18, 24, or 48 hours in the time course experiments, then permeabilized (25). The cells were labeled with MycN antibodies by successive incubations with 1 μg/mL anti-MycN antibodies, 5 μg/mL biotin goat anti-rat IgG (Jackson Immuno Research), and 0.5 μg/mL Cy3-streptavidin (Jackson ImmunoResearch) as detailed earlier (25). For background staining, samples were stained in the absence of MycN antibodies. Staining intensity was analyzed with a Zeiss LSM 510 confocal microscope fitted with nonleaking green and red fluorescence filters (25).

Sequence analysis of MycN gene box 1. RNA was extracted from LAN-1 cells using the SV Total RNA Isolation System (Promega, Madison, WI). RT-PCR was done with a Qiagen kit according to the instructions in the manual (Hilden, Germany), using the forward 5′-ATG CCG GGC ATG ATC TGC AAG AAC CC-3′ primer and the reverse 5′-GGG CGG TGG AAC CGG CGG TTG GC GG-3′ primer. The 368 bp RT-PCR product was subcloned into pGEM-T easy vector (Promega) and sequenced.

Gene expression profiling. All experiments were done using Affymetrix Human Focus oligonucleotide arrays, as described at http://www.affymetrix.com/support/technical/datasheets/human_datasheet.pdf. Total RNA from each sample was used to prepare biotinylated target RNA. A complete description of the procedures is available at http://bioinf.picr.man.ac.uk/mbcf/downloads/GeneChip_Target_-Prep_Protocol_CRUK_v_2.pdf. The target cRNA was then generated from each sample according to the manufacturer's instructions, using an Affymetrix GeneChip Instrument System (Affymetrix, Santa Clara, CA). Spike controls were added to 10 μg of fragmented cRNA prior to overnight hybridization. Arrays were then washed and stained with streptavidin-phycoerythrin before being scanned on an Affymetrix GeneChip scanner. Details of quality control measures can be found in Supplementary Table S3. Genes were analyzed using the Mas 5 algorithm (see pivot data in Supplementary Table S1). Genes were filtered see Supplementary Table S2; samples of farnesylthiosalicylic acid – treated cells were compared with samples of untreated cells and differentially expressed genes were selected using *t* test with a threshold *P* value of 0.05. Genes were classified into functional groups using the GO annotation tool (http://apps1.niaid.nih.gov/David/upload.asp; ref. 26).

Real-time PCR for the determination of RBBP1 expression levels. Extracts of total RNA (1 μg) from cells treated for 48 hours with farnesylthiosalicylic acid (50 μmol/L) or vehicle (control) were reverse-transcribed in a total volume of 20 μL using the iSCRIPT cDNA Kit (Bio-Rad, Hercules, CA). The cDNA samples were then used for real-time PCR (Syber Green PCR Kit, Roche, Nutley, NJ). The PCR conditions and the primers used for RBBP1 and for the housekeeping genes glyceraldehyde-3-phosphate dehydrogenase and HMBS are detailed in the supplement, real-time PCR table (http://eng.sheba.co.il/genomics).

Results

LAN-1 cells display active Ras and Ras pathways that contribute to their malignant phenotype. To investigate the possibility that MycN and active Ras cooperatively contribute to the malignant phenotype of aggressive neuroblastoma, we

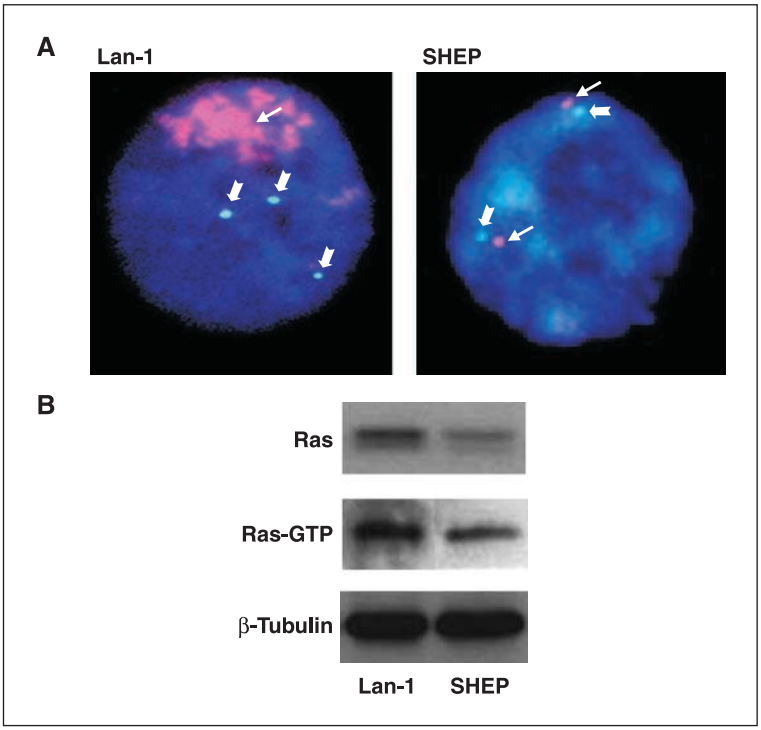

Fig. 1. LAN-1 cells exhibit amplified *MycN* gene and high levels of active Ras. *A*, fluorescence *in situ* hybridization analysis of LAN-1 and SHEP cells shows cells in interphase. Bold arrows, centromeres of chromosome 2 are in green; thin arrows, two copies of the *MycN* gene in the SHEP cell line and the amplified *MycN* gene in LAN-1 cells are in red. *B*, difference in basal expression of Ras and Ras-GTP in LAN-1 and SHEP cell lines. The cells were homogenized, and aliquots of the cell homogenates were subjected to the determination of levels of Ras and Ras-GTP (by glutathione S-transferase – Ras-binding domain pull-down) using SDS-PAGE and immunoblotting with anti-Ras or anti-β-tubulin antibodies (loading control). Typical immunoblots are shown. SHEP cells exhibited, respectively, (means ± SD, $n = 3$), 49 ± 8% and 62 ± 3.5% lower levels of Ras and Ras-GTP as compared with LAN-1 cell ($P < 0.01$).

chose the LAN-1 cell line, known to possess amplified *MycN* gene (18). Possession of this amplified gene was confirmed by fluorescence *in situ* hybridization analysis, with human neuroblastoma SHEP cells devoid of amplified *MycN* (27) used as a control (Fig. 1A). Separate experiments showed that significantly larger amounts of Ras and Ras-GTP are exhibited by LAN-1 cells than by SHEP cells (Fig. 1B). The first indication that active Ras might be required for the malignant expression of the amplified *MycN* gene came from experiments with the Ras inhibitor farnesylthiosalicylic acid (20, 21). This compound inhibited the growth of LAN-1 cells (Fig. 2A, B, and C). Under the conditions employed in these experiments, farnesylthiosalicylic acid had no cytotoxic effects, as indicated by Hoechst dye exclusion staining (Fig. 2A and B). Inhibition of LAN-1 cell growth by farnesylthiosalicylic acid was dose-dependent with growth inhibition of 50% at 35 μmol/L farnesylthiosalicylic acid (Fig. 2C). The Ras inhibitor also induced a significant change in cell morphology, manifested by flattening of the cells (Fig. 2C, inset).

Over the concentration range at which farnesylthiosalicylic acid inhibited cell growth (50 μmol/L), it induced a small nonsignificant decrease of (mean ± SD, $n = 3$) 24 ± 9.1% in total Ras, a significant decrease of 30 ± 6.9% ($P < 0.01$) in membrane-associated (P_{100}) Ras, and a stronger decrease of 47 ± 8.5% ($P < 0.01$) in Ras-GTP (Fig. 3A). The farnesylthiosalicylic acid–induced decrease in active Ras in the LAN-1 cells was accompanied by a decline in Ras signaling to Raf-1-MEK-ERK and to PI3K-Akt. Farnesylthiosalicylic acid inhibited Raf-1 activity by 24 ± 10% (mean ± SD, $n = 3$, $P < 0.05$) and caused a reduction of 36 ± 6.6% ($P < 0.05$) in active pERK (Fig. 3A and B). Inhibition of PI3K activity (by 41 ± 13%, $P < 0.05$; Fig. 3C) and reduction in active pAkt (by 59 ± 7.4%, $P < 0.001$; Fig. 3A) were significantly stronger than the inhibition of Raf-1 activity and the reduction in pERK.

Next, we examined the effects of farnesylthiosalicylic acid on prominent regulators of the cell cycle. Within 24 to 48 hours farnesylthiosalicylic acid induced the down-regulation of cyclin D1 and of hyperphosphorylated retinoblastoma and E2F1, and concomitant up-regulation of the Cdk inhibitor p27 (Fig. 4A). The decreases in cyclin D1, in phosphorylated retinoblastoma and in E2F1 at 48 hours (mean ± SD, $n = 3$) were, respectively, 34 ± 8%, 32 ± 9%, and 44 ± 17%. The increase in p27 at 48 hours was 1.3 ± 0.15-fold (mean ± SD, $n = 3$). Interestingly, in a gene profiling experiment (described below), we found that farnesylthiosalicylic acid induced a 4.3-fold increase in expression of the RBBP1, which inhibits E2F1 transcriptional activity (28). This observation was confirmed by real-time PCR analysis, which disclosed a 1.4-fold increase in RBBP1 expression as a result of the farnesylthiosalicylic acid treatment. Using specific anti-RBBP1 antibodies, we found that farnesylthiosalicylic acid induced a 58 ± 10% (mean ± SD, $n = 3$) increase in expression of the RBBP1 protein ($P < 0.05$, Fig. 4B). Taken together, the results can explain the

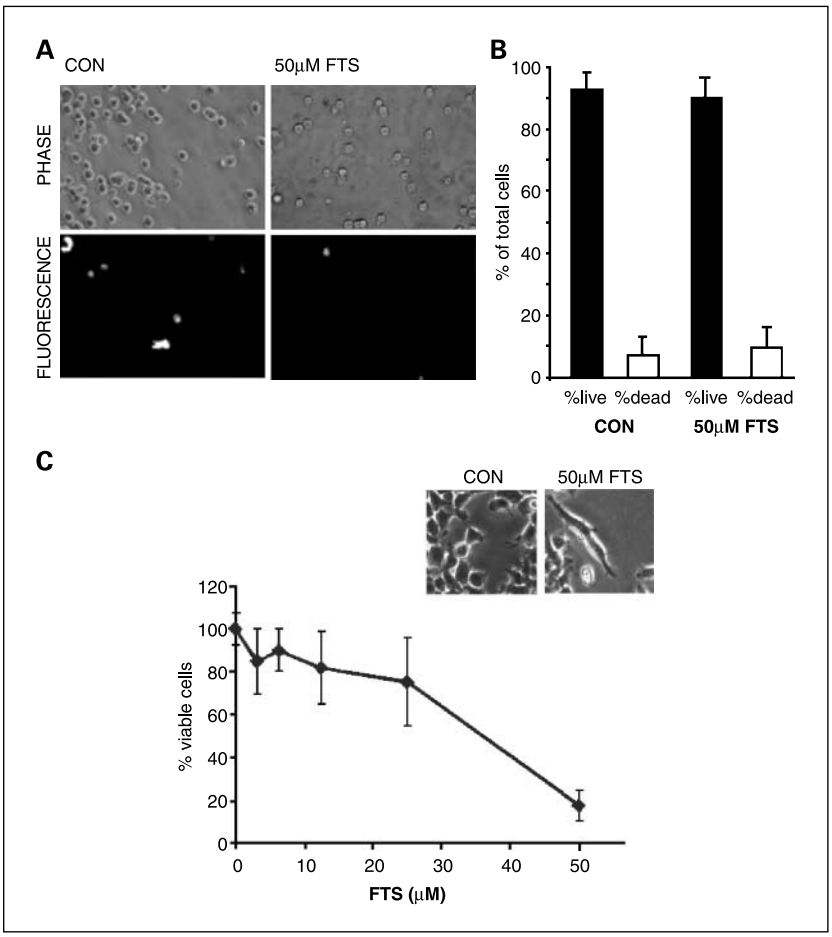

Fig. 2. The Ras inhibitor farnesylthiosalicylic acid inhibits growth of LAN-1 cells possessing an amplified *MycN* gene. *A*, Hoechst dye exclusion staining of control and farnesylthiosalicylic acid – treated LAN-1 cells. The cells were incubated for 5 days in the absence and in the presence of 50 μmol/L farnesylthiosalicylic acid, then stained with Hoechst 33258, as described in Materials and Methods, and visualized under a fluorescence microscope (×10). Typical phase and fluorescence images are shown. Images recorded in four distinct fields in each of five separate wells were quantified by counting the total number of cells and the number of fluorescently labeled (dead) cells. *B*, number of dead cells, calculated as a percentage of the total number of cells (means ± SD, $n = 10$). *C*, cells were incubated for 5 days in the absence and in the presence of the indicated concentrations of farnesylthiosalicylic acid, then detached from the plates and counted. The numbers of cells in drug-treated samples, calculated as a percentage of the total number of cells in the control (means ± SD, $n = 4$), are shown. Inset, morphologic changes in treated cells compared with control cells (×20).

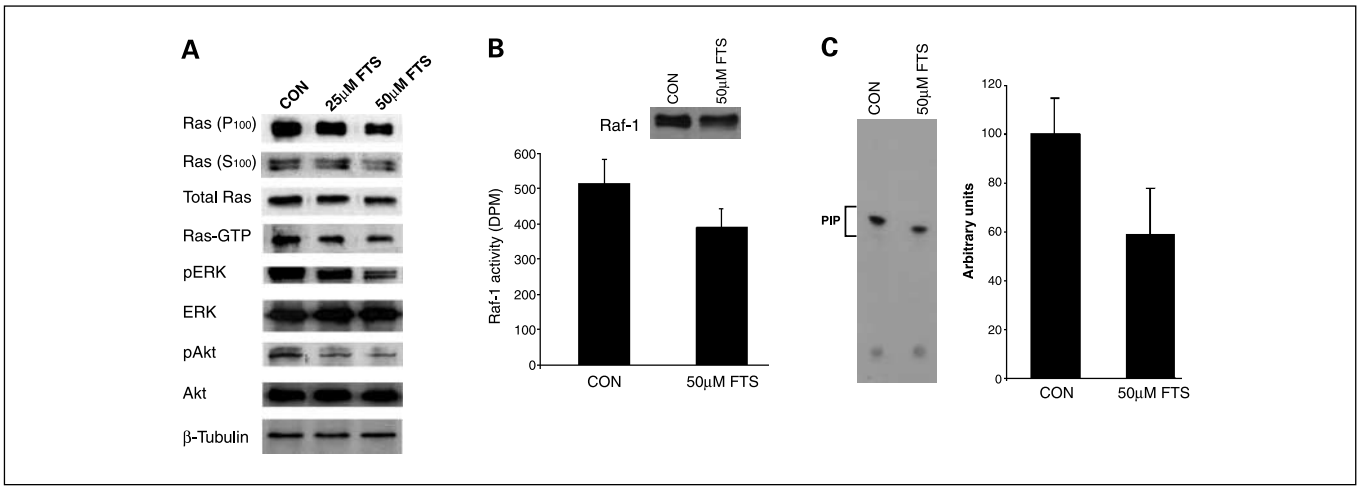

Fig. 3. Farnesylthiosalicylic acid reduces the amounts of active Ras and inhibits Ras signaling to the Raf-MEK-ERK and PI3K-Akt pathways. LAN-1 cells were incubated for 48 hours in the absence and in the presence of the indicated concentrations of farnesylthiosalicylic acid. *A*, the cells were then homogenized, and aliquots of the cell homogenates were subjected to glutathione S-transferase – Ras-binding domain pull-down followed by SDS-PAGE and immunoblotting with anti-Ras or were immunoblotted with anti-phospho-ERK, anti-ERK, anti-phospho-Akt, anti-Akt, and anti-β-tubulin antibodies. Typical immunoblots are shown. *B*, Raf-1 activity in the cell lysates. Mean values of Raf-1 activity (±SD) from three independent experiments. C, PI3K activity in the cell lysates. Results of a representative experiment (phosphatidyl inositol-3-phosphate spots detected on an X-ray film), and their quantification (mean ± SD, $n = 4$) are shown.

observed farnesylthiosalicylic acid inhibition of LAN-1 cell proliferation.

Farnesylthiosalicylic acid or dominant-negative Ras induce a dramatic decrease in MycN and disappearance of MycN from nuclei of LAN-1 cells. Next, we examined whether LAN-1 cells express significant amounts of the MycN protein, and if so, how this protein is affected by Ras inhibition. LAN-1 cells were incubated for 48 hours with or without farnesylthiosalicylic acid (25 and 50 μmol/L) and then immunoblotted with specific anti-MycN antibodies. Results of typical immunoblots (Fig. 5A) show that LAN-1 cells expressed relatively large amounts of MycN, which were strongly down-regulated by 50 μmol/L farnesylthiosalicylic acid (65 ± 8% decrease; mean ± SD, $n = 3$, $P < 0.01$). Immunofluorescence analysis confirmed these results and showed that in the control cells, MycN was localized almost exclusively to the large nuclei (red, cy3 fluorescence), from which the drug treatment caused its complete removal (Fig. 5B). The small amount of MycN that remained after the treatment was found in the cytosol (Fig. 5B). To confirm that this effect was indeed related to the farnesylthiosalicylic acid–induced down-regulation of active Ras, we used Ras17N, a dominant-negative Ras isoform. The cells were cotransfected with vectors encoding GFP (to enable identification of the transfected cells) and Ras17N or with GFP and the empty vector control. Typical dual fluorescence images (green fluorescence, GFP; red fluorescence, MycN) from these experiments showed that Ras17N induced complete removal of MycN from the nuclei with no accumulation of MycN in the cytosol (Fig. 5C), a finding indistinguishable from that of the effect of the Ras inhibitor farnesylthiosalicylic acid.

The farnesylthiosalicylic acid–induced mislocalization of MycN was time-dependent: a significant effect was observed not earlier than 18 hours after exposure, and was stronger 24 and 48 hours after the drug treatment (Fig. 6). Taken together, these experiments showed that the presence of large amounts of nuclear MycN in LAN-1 cells depends on the presence of active Ras-GTP, presumably because Ras stabilizes the MycN protein.

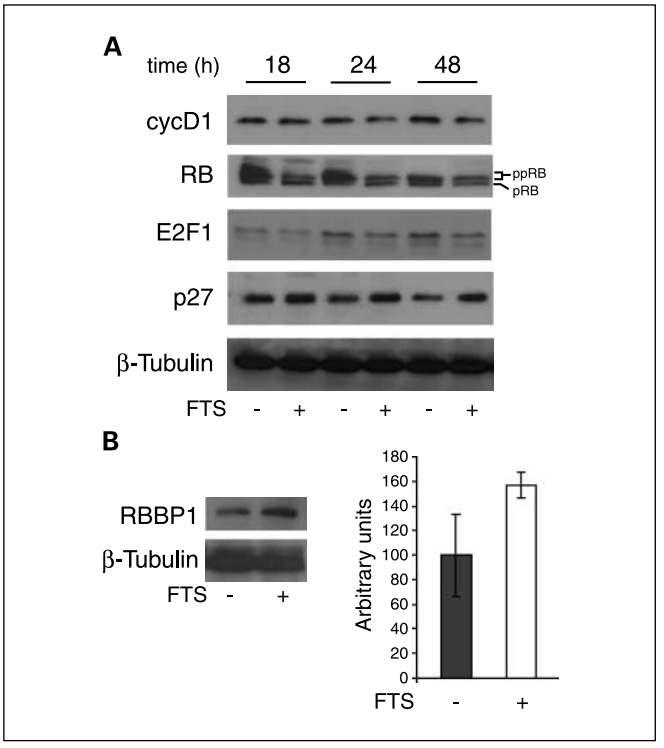

Fig. 4. *A*, farnesylthiosalicylic acid treatment induces time-dependent alterations in retinoblastoma, cyclin D1, E2F1, and p27 in LAN-1 cells. LAN-1 cells were plated (1.5×10^6 cells/10 cm plate) and treated with the solvent or 50 μmol/L farnesylthiosalicylic acid for the indicated time periods. The cells were then lysed and subjected to SDS-PAGE and immunoblotting with anti-cyclin D1, anti-retinoblastoma, anti-E2F1, and anti-p27 antibodies. The experiment was repeated thrice and typical immunoblots visualized by enhanced chemiluminescence are shown. pRB, phosphorylated retinoblastoma; ppRB, hyperphosphorylated retinoblastoma. The decreases in cycline D1 and in phosphorylated retinoblastoma at 48 hours were statistically significant ($P < 0.05$). The increase in p27 at 48 hours and the decrease in E2F1 did not gain statistical significance. *B*, farnesylthiosalicylic acid induces an increase in the levels of RBBP1. LAN-1 cells were plated (1.5×10^6 cells/10 cm plate) and then treated with 0.1% Me_2SO or 50 μmol/L farnesylthiosalicylic acid for 48 hours. The cells were lysed and subjected to SDS-PAGE and immunoblotting using anti-RBBP1 antibodies.

Farnesylthiosalicylic acid promotes MycN degradation through the proteasome pathway. Next we examined whether the maintenance of large amounts of MycN in LAN-1 cells is associated with Ras-dependent phosphorylation and stabilization of MycN. Standard RT-PCR and sequencing procedures (see Materials and Methods) confirmed that the relevant MycN phosphorylation sites namely, Thr^{58} and Ser^{62}, were not mutated in LAN-1 cells. This indicated that the observed Ras-dependent stabilization of MycN (Figs. 6 and 7) might be achieved, at least in part, by the Ras/PI3K/Akt pathway that prevents GSK-3-mediated phosphorylation of Thr^{58}, a process that targets Myc to ubiquitin-mediated proteosomal degradation (1, 8).

To examine this possibility, we incubated LAN-1 cells with farnesylthiosalicylic acid to down-regulate the active p-Akt protein (Fig. 3) and then determined the amount of p-MycN. The cells were exposed to farnesylthiosalicylic acid for 3 hours and then lysed, and the lysates were immunoblotted with specific anti-phospho-MycN (Thr^{58}/Ser^{62}) antibodies. As shown in Fig. 7A, the Ras inhibitor induced a significant increase in p-MycN. This is consistent with the proposed mechanism whereby lack of Akt-mediated phosphorylation of GSK-3 promotes GSK-mediated phosphorylation of MycN. This notion was further supported by the finding that LiCl, which inhibits GSK-3 activity (29), blocked the farnesylthiosalicylic acid–induced increase in p-MycN (Fig. 7A, left). In addition LY294002, which inhibits PI3K, induced a significant increase in p-MycN (Fig. 7A, right). The MEK inhibitor U0126 induced a small insignificant decrease in p-MycN (Fig. 7, right). Notably, no apparent change in the total amount of MycN was observed in these experiments (Fig. 7A) consistent with our earlier observation that MycN was down-regulated only 18 hours after farnesylthiosalicylic acid treatment (Fig. 6). Thus, the observed farnesylthiosalicylic acid–induced phosphorylation of MycN preceded MycN down-regulation. This picture is consistent with a consecutive mechanism, previously known in the case of c-Myc, in which Thr^{58} is phosphorylated and this targets c-Myc to proteosomal degradation. We therefore examined the effect of the proteasome inhibitor MG132 (30) on farnesylthiosalicylic acid–induced down-regulation of MycN. For these experiments, we chose a protocol in which the cells were incubated with farnesylthiosalicylic acid for a relatively long period (18 hours), at which MycN down-regulation was already apparent. Consistent with the results shown in Fig. 7, farnesylthiosalicylic acid indeed induced a decrease in the amounts of both MycN and p-MycN (Fig. 7B). At the same time, LAN-1 cells were incubated for 12 hours with farnesylthiosalicylic acid alone (to prime MycN phosphorylation and degradation), and then for a further 6 hours with farnesylthiosalicylic acid and MG132. Basal activity was determined in cells that were treated for 12 hours with the vehicle and for an additional 6 hours with MG132. As shown in Fig. 7B, MG132 blocked both the basal and the farnesylthiosalicylic acid–induced degradation of p-MycN. Thus, it seems that MycN, like c-Myc (1, 8), was degraded by the proteasome. Accordingly, the observed down-regulation of MycN by farnesylthiosalicylic acid was evidently an outcome of enhanced phosphorylation (Fig. 7A) and proteasomal degradation of the protein (Fig. 7B). These conclusions were strengthened by the observation that MG132 inhibited the farnesylthiosalicylic acid–induced disappearance of MycN from the nuclei of LAN-1 cells (Fig. 7C).

Profiling of gene expression in farnesylthiosalicylic acid–treated LAN-1 cells. Next we examined whether the farnesylthiosalicylic acid–induced down-regulation of MycN in

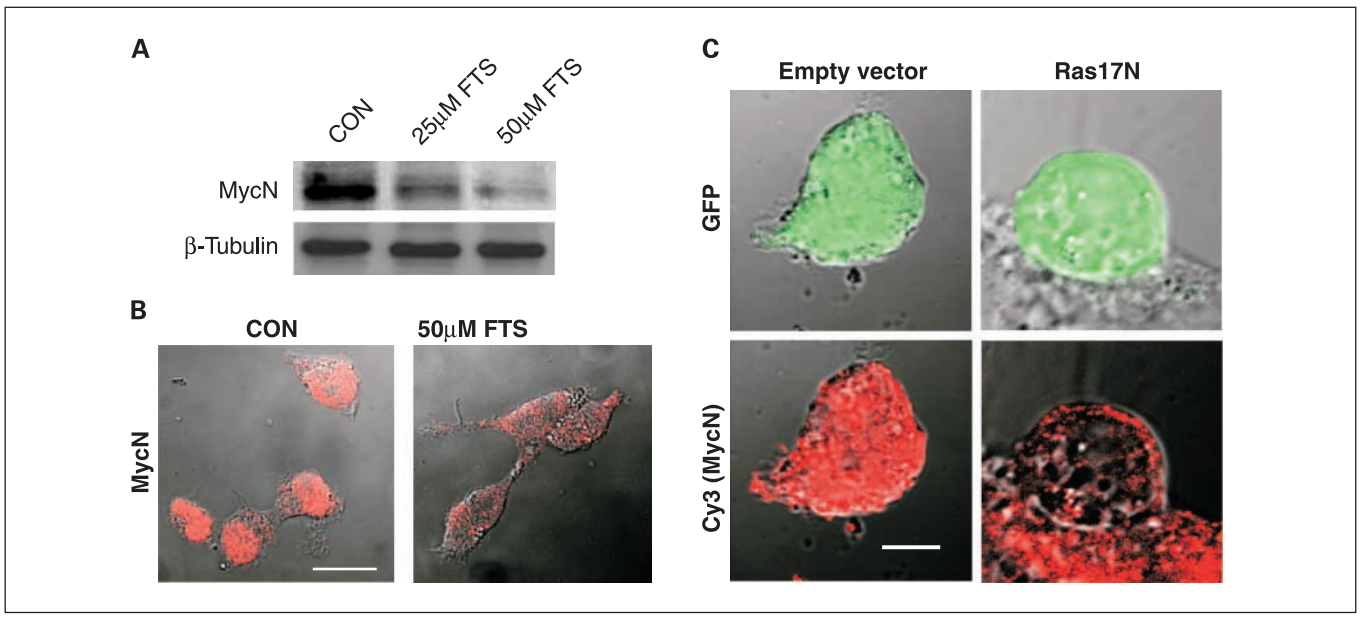

Fig. 5. Both dominant-negative Ras and farnesylthiosalicylic acid down-regulate MycN protein in LAN-1 cells. LAN-1 cells were incubated for 48 hours in the absence and in the presence of the indicated concentrations of farnesylthiosalicylic acid. *A*, the cells were then homogenized, and aliquots of the cell homogenates were subjected to SDS-PAGE and immunoblotting with anti-MycN and anti-β-tubulin antibodies. Typical immunoblots visualized by enhanced chemiluminescence. *B*, the cells were fixed, permeabilized, labeled with anti-MycN antibodies, and then incubated with biotin goat anti-mouse IgG and Cy3-streptavidin. Profiles of fluorescence staining were recorded with a Zeiss LSM 510 confocal microscope. Typical images are shown (*bar*, 20 μm). Similar results were obtained in three independent experiments. *C*, LAN-1 cells were cotransfected with plasmid DNA coding for Ras17N (1.4 μg) or with a control vector (PCDNA; 1.4 μg) along with plasmid DNA coding for GFP (0.6 μg). After 48 hours, the cells were fixed, permeabilized, and labeled as described in (*B*). Profiles of fluorescence staining (green for GFP, red for Cy3) were recorded with a Zeiss LSM 510 confocal microscope fitted with fluorescein and rhodamine filters. Bar, 20 μm. Typical images are shown. Similar results were obtained in two independent experiments.

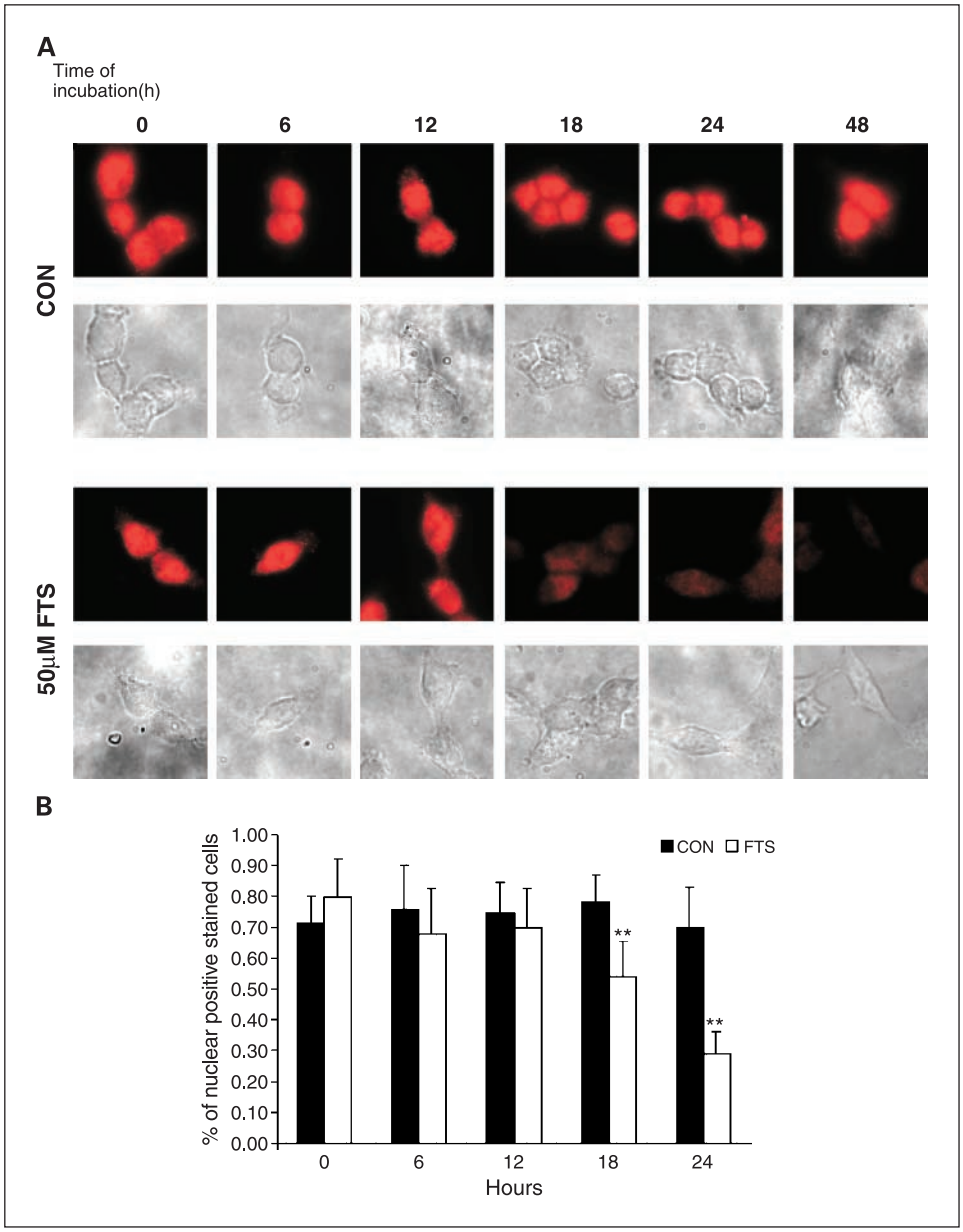

Fig. 6. Time-dependent reduction in MycN protein induced by farnesylthiosalicylic acid in LAN-1 cells. LAN-1 cells were plated (1×10^5 cells per well in six-well plates) and treated with 0.1% Me_2SO or 50 μmol/L farnesylthiosalicylic acid for the indicated time periods. *A*, cells were then fixed, permeabilized, labeled with anti-MycN antibodies, and incubated with biotin-goat anti-mouse IgG and Cy3-streptavidin. The cells were then visualized under a fluorescence microscope (×63). Typical fluorescence and phase images are shown. *B*, percentages of farnesylthiosalicylic acid – treated and control cells showing nuclear MycN staining (mean ± SD, $n = 10$). **, $P < 0.001$, *t* test. Bar, 20 μm.

LAN-1 cells affects the expression of genes controlled by MycN. Because MycN regulates the expression of a large number of genes (31), we chose a comprehensive approach and gene expression analysis was done. We incubated LAN-1 cells with 50 μmol/L farnesylthiosalicylic acid or with the control vehicle for 18, 24, or 48 hours and then processed them for analysis of DNA microarray gene expression using the Affymetrix Human Genome Focus Array (8,500 sequences), as described in Materials and Methods. Analysis of the data using the Mas 5 algorithm (32) yielded a list of 4,799 "valid genes" (see Materials and Methods and supplementary Table S2), of which 211 showed significantly increased or decreased expression (control versus farnesylthiosalicylic acid, $P < 0.05$) at one or more time points during the drug treatment. Using the GO annotation tool (26) we then did functional clustering analysis (Fig. 8), which enabled us to identify three large groups of genes whose expression was altered by the drug treatment. These included genes involved in signal transduction, genes involved in nucleotide and nucleic acid metabolism, and genes involved in protein metabolism (Fig. 8). Because MycN enhances the expression of genes involved in ribosome biogenesis and protein synthesis (31), these kinds of alterations are clearly consistent with loss of MycN transcriptional activity. Further analysis of the gene expression profiles is needed and will be described elsewhere.

Discussion

MycN gene amplification is frequently detected in aggressive neuroblastoma (15, 33). Strong expression of MycN protein, together with the presence of active Ras, could contribute to the malignant phenotype of these tumors as a result of cooperation between Ras and MycN. Up to now, this possibility has not been directly addressed. LAN-1 cells

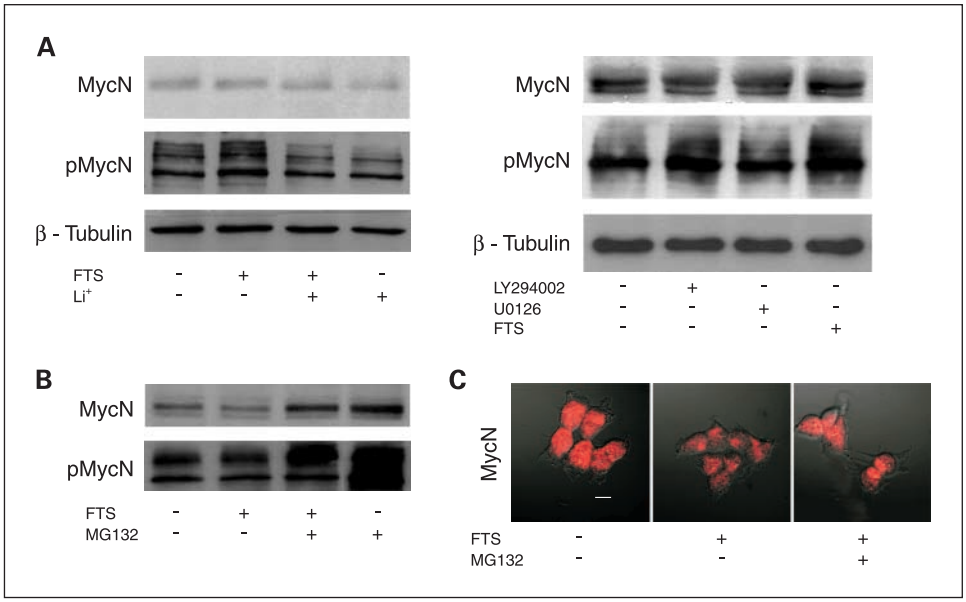

Fig. 7. The farnesylthiosalicylic acid – induced increase in MycN phosphorylation, which is blocked by LiCl, facilitates MG132-blockable degradation of MycN. *A*, LAN-1 cells were plated (1.5×10^6 cells/10 cm plate) and treated with 0.1% Me_2SO or 50 μmol/L farnesylthiosalicylic acid, with or without 20 mmol/L LiCl (left). The cells were also incubated with or without 50 μmol/L LY294002 or 40 μmol/L U0126 or 50 μmol/L farnesylthiosalicylic acid for 3 hours (right). The cells were lysed and subjected to SDS-PAGE and immunoblotting with anti-MycN, anti-phospho-MycN and anti-β-tubulin antibodies. Note that the increase in pMycN (1.4 ± 0.08; means ± SD, $n = 3$; $P < 0.01$) in the presence of farnesylthiosalicylic acid was blocked by addition of LiCl. LY294002 induced a 1.3 ± 0.04 increase in pMycN (means ± SD, $n = 3$; $P < 0.01$) whereas the effect of U0126 was insignificant. The total amount of MycN did not change. *B*, LAN-1 cells were plated (1.5×10^6 cells/10 cm plate) and treated with 0.1% Me_2SO or 50 μmol/L farnesylthiosalicylic acid, with or without 50 μmol/L MG132, the proteasome inhibitor. The total incubation time was 18 hours. In the experiments in which MG132 was added, cells were incubated with farnesylthiosalicylic acid or Me_2SO for 12 hours only, and for a further 6 hours with MG132. They were then lysed and subjected to SDS-PAGE and immunoblotting with anti-MycN and anti-pMycN antibodies. Note the decrease in total MycN and pMycN in the presence of farnesylthiosalicylic acid. MG132 blocked both the basal and the farnesylthiosalicylic acid – induced degradation of pMycN. *C*, LAN-1 cells were plated (six-well plates, 1×10^5 cells per well) and treated as described in (*B*). They were then fixed, permeabilized, labeled with anti-MycN antibodies, and incubated with biotin-goat anti-mouse IgG and Cy3-streptavidin. The cells were then analyzed for MycN by fluorescence confocal microscopy. Bar, 20 μm. Typical fluorescence and phase images are shown. Similar results were obtained in two separate experiments.

possessing amplified *MycN* gene (ref. 18; see Fig. 1A) exhibit growth advantage and are more aggressive as compared with neuroblastoma lines which possess a lower number of *MycN* gene copies or do not express MycN (34–36). Here we showed that LAN-1 cells exhibited significant amounts of active Ras-GTP, whose down-regulation by the Ras inhibitor farnesylthiosalicylic acid (Fig. 3) resulted in a dramatic decrease in MycN protein (Figs. 5 and 6). The specificity of

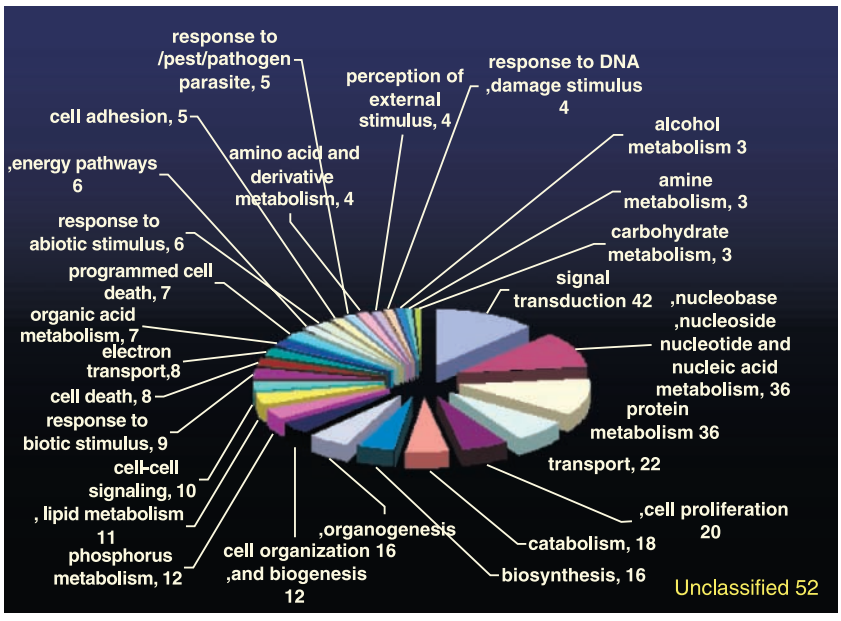

Fig. 8. Microarray profiling of gene expression in farnesylthiosalicylic acid – treated LAN-1 cells. LAN-1 cells were plated (1.5×10^6 cells/10 cm plate), and treated with 0.1% Me_2SO or 50 μmol/L farnesylthiosalicylic acid for 18, 24, or 48 hours. We then processed the cells for RNA extraction and microarray profiling using the Human Genome Focus Array. Results of the functional clustering analysis as detailed in Materials and Methods. The three major groups of genes whose expression was altered after farnesylthiosalicylic acid treatment were genes involved in signal transduction, in nucleotide and nucleic acid metabolism, and protein metabolism.

this effect was confirmed by transfection of LAN-1 cells with dominant-negative Ras, which induced MycN down-regulation (Fig. 5C) that was indistinguishable from that induced by the Ras inhibitor. Thus, the amplified *MycN* gene by itself is not sufficient to maintain large amounts of MycN in the nuclei of LAN-1 cells, and Ras expression and activation seem to be required as well.

Consistent with the known mechanisms of c-Myc stabilization by oncogenic Ras (8), we found that down-regulation of Ras-GTP by farnesylthiosalicylic acid resulted in an increase in MycN phosphorylation, which was blocked by LiCl, an inhibitor of GSK-3 (29). Because GSK-3 phosphorylates Thr^{58}, which is required for Myc degradation (8), this finding strongly suggested that the Ras inhibitor enhances the phosphorylation of Thr^{58} of the MycN protein. In line with this suggestion, we found that the activity of PI3K and the amounts active p-Akt were down-regulated by Ras inhibition (Fig. 3), thus preventing the inhibitory action of p-Akt on GSK-3 (1). Indeed, the PI3K inhibitor LY294002, like farnesylthiosalicylic acid, induced an increase in pMycN (Fig. 7). Moreover, it seems that the Thr^{58}-phosphorylated MycN, like Thr^{58}-phosphorylated c-Myc (1, 8), is degraded by the proteasome pathway because the proteasome inhibitor MG132 blocked both basal and farnesylthiosalicylic acid–induced MycN degradation in LAN-1 cells (Fig. 7).

The farnesylthiosalicylic acid–induced facilitation of MycN degradation (Fig. 7B and C) resulted in the disappearance of MycN from the nuclei of LAN-1 cells. This shows that it is sufficient to block Ras activity in LAN-1 cells in order to disrupt both Ras signals and MycN transcriptional activity. Treatment of LAN-1 cells with farnesylthiosalicylic acid indeed resulted in marked alterations in the cell cycle machinery proteins regulated by Ras and by Myc. The observed decrease in the amounts of cyclin D1, phospho-retinoblastoma, and E2F after farnesylthiosalicylic acid treatment (Fig. 4A) can be attributed to the known mechanisms of Ras regulation of cyclin D1/Cdk4 (1, 9–11), namely the Raf-MEK-ERK cascade, shown to promote increased expression of cyclin D1 and assembling of the active cyclin D1/Cdk4 complex (37), and the PI3K-Akt pathway, shown to prevent degradation of cyclin D1 by the Akt-mediated inhibitory phosphorylation of GSK-3, which in its unphosphorylated form tags cyclin D1 for ubiquitin/proteasome degradation (38). The expected outcome of ERK and Akt inhibition (Fig. 3A) is then the down-regulation of cyclin D1 (Fig. 4A). This, together with the increase in p27 that blocks cyclin E/Cdk2 activity, would seem to account for the decrease in hyperphosphorylated retinoblastoma (Fig. 4A), because both the initial cyclin D1/Cdk4-dependent phosphorylation and the subsequent cyclin E/Cdk2-dependent phosphorylation of retinoblastoma would be prevented. This would lead in turn to reduction in the expression of E2F (Fig. 4A).

In addition to the decrease in E2F observed in the farnesylthiosalicylic acid–treated cells, we observed a significant increase in the expression of RBBP1. This protein, known as a pocket protein of retinoblastoma, acts as an adaptor that recruits histone deacetylase to a complex with mSIN3. Association of RBBP1-histone deacetylase-mSIN3 complex with the retinoblastoma pocket results in the inhibition of E2F transcriptional activity (28). Altogether, it seems then that farnesylthiosalicylic acid–treated LAN-1cells enter a phase in which positive effectors of cell cycle progression are down-regulated and negative effectors are up-regulated.

The mechanism of the farnesylthiosalicylic acid–induced increase in p27 in LAN-1 cells is not yet clear. It is not associated with the tumor suppressors p73 and p53, which would up-regulate p27 expression, because LAN-1 cells do not express p73 or p53 (39). The mechanism of RBBP1 up-regulation by farnesylthiosalicylic acid seems to be associated with the direct inhibition of Ras. Activated K-Ras was recently shown to down-modulate the formation of retinoblastoma/RBBP1 complex by reducing *RBBP1* gene expression (40). These experiments, which show that Ras signaling attenuates RBBP1 expression, are in line with our present observation that Ras inhibition induced up-regulation of RBBP1.

Finally, the farnesylthiosalicylic acid–induced loss of active Ras and of MycN protein in LAN-1 cells was clearly manifested in profiles of gene expression that could be expected from the loss of MycN transcriptional activity and of Ras signaling (31). For example, we observed changes in the expression of genes that are involved in ribosome biogenesis and protein synthesis (Fig. 8). These findings are in line with the results of a recent analysis of gene expression in Ras-transformed cells, Myc-transformed cells, and a variety of human tumor cells (41). The analysis showed that the profiles of gene expression in tumors with high expression of c-Myc are consistent with the profiles in tumors that express dysfunctional Ras (41). This is apparently due to the fact that both types of tumors exhibit activated Ras (41). The accumulated findings, taken together with the present experiments, suggest that Ras inhibitors that cancel the cooperation between Myc and Ras are valuable candidates for the treatment of human tumors with high expression of Myc, such as neuroblastoma type III.

Acknowledgments

We thank S.R. Smith for editorial assistance and B. Rotblat for his contribution in MycN sequencing.

References

1. Sears RC, Nevins JR. Signaling networks that link cell proliferation and cell fate. J Biol Chem 2002;277:11617–20.
2. Bourne HR, Sanders DA, McCormick F. The GTPase superfamily: conserved structure and molecular mechanism. Nature 1991;349:117–27.
3. Shields JM, Pruitt K, McFall A, Shaub A, Der CJ. Understanding Ras: 'it ain't over 'til it's over'. Trends Cell Biol 2000;10:147–54.
4. Bos JL. Ras oncogenes in human cancer: a review. Cancer Res 1989;49:4682–9.
5. Basu TN, Gutmann DH, Fletcher JA, et al. Aberrant regulation of ras proteins in malignant tumour cells from type 1 neurofibromatosis patients. Nature 1992;356:713–5.
6. Suhardja A, Kovacs K, Rutka J. Genetic basis of pituitary adenoma invasiveness: a review. J Neurooncol 2001;52:195–204.
7. Claassen GF, Hann SR. Myc-mediated transformation: the repression connection. Oncogene 1999;18:2925–33.
8. Sears R, Nuckolls F, Haura E, et al. Multiple Ras-dependent phosphorylation pathways regulate Myc protein stability. Genes Dev 2000;14:2501–14.
9. Yordy JS, Muise-Helmericks RC. Signal transduction and the Ets family of transcription factors. Oncogene 2000;19:6503–13.
10. Filmus J, Robles AI, Shi W, et al. Induction of cyclin D1 overexpression by activated ras. Oncogene 1994;9:3627–33.
11. Pruitt K, Der CJ. Ras and Rho regulation of the cell cycle and oncogenesis. Cancer Lett 2001;171:1–10.

12. Facchini LM, Penn LZ. The molecular role of Myc in growth and transformation: recent discoveries lead to new insights. FASEB J 1998;12:633–51.

13. Yeh E, Cunningham M, Arnold H, et al. A signalling pathway controlling c-Myc degradation that impacts oncogenic transformation of human cells. Nat Cell Biol 2004;6:308–18.

14. D'Cruz CM, Gunther EJ, Boxer RB, et al. c-MYC induces mammary tumorigenesis by means of a preferred pathway involving spontaneous Kras2 mutations. Nat Med 2001;7:235–9.

15. Schwab M. Human neuroblastoma: from basic science to clinical debut of cellular oncogenes. Naturwissenschaften 1999;86:71–8.

16. Schmidt ML, Lukens JN, Seeger RC, et al. Biologic factors determine prognosis in infants with stage IV neuroblastoma: a prospective Children's Cancer Group study. J Clin Oncol 2000;18:1260–8.

17. Moley JF, Brother MB, Wells SA, et al. Low frequency of ras gene mutations in neuroblastomas, pheochromocytomas, and medullary thyroid cancers. Cancer Res 1991;51:1596–9.

18. Kohl NE, Gee CE, Alt FW. Activated expression of the N-myc gene in human neuroblastomas and related tumors. Science 1984;226:1335–7.

19. Nakagawara A, Azar CG, Scavarda NJ, Brodeur GM. Expression and function of TRK-B and BDNF in human neuroblastomas. Mol Cell Biol 1994;14:759–67.

20. Haklai R, Gana-Weisz G, Elad G, et al. Dislodgment and accelerated degradation of Ras. Biochemistry 1998;37:1306–14.

21. Kloog Y, Cox AD, Sinensky M. Concepts in Ras-directed therapy. Expert Opin Investig Drugs 1999;8:2121–40.

22. Cohen N, Novikov I, Hardan I, et al. Standardization criteria for the detection of BCR/ABL fusion in interphase nuclei of chronic myelogenous leukemia patients by fluorescence *in situ* hybridization. Cancer Genet Cytogenet 2000;123:102–8.

23. Elad-Sfadia G, Haklai R, Ballan E, Gabius HJ, Kloog Y. Galectin-1 augments Ras activation and diverts Ras signals to Raf-1 at the expense of phosphoinositide 3-kinase. J Biol Chem 2002;277:37169–75.

24. Herrmann C, Martin GA, Wittinghofer A. Quantitative analysis of the complex between p21ras and the Ras-binding domain of the human Raf-1 protein kinase. J Biol Chem 1995;270:2901–5.

25. Niv H, Gutman O, Henis YI, Kloog Y. Membrane interactions of a constitutively active GFP-K-Ras 4B and their role in signaling: evidence from lateral mobility studies. J Biol Chem 1999;274:1606–13.

26. Dennis G Jr, Sherman BT, Hosack DA, et al. DAVID: Database for Annotation, Visualization, and Integrated Discovery. Genome Biol 2003;4:P3.

27. Hopkins-Donaldson S, Yan P, Bourloud KB, et al. Doxorubicin-induced death in neuroblastoma does not involve death receptors in S-type cells and is caspase-independent in N-type cells. Oncogene 2002;21:6132–7.

28. Lai A, Kennedy BK, Barbie DA, et al. RBP1 recruits the mSIN3-histone deacetylase complex to the pocket of retinoblastoma tumor suppressor family proteins found in limited discrete regions of the nucleus at growth arrest. Mol Cell Biol 2001;21:2918–32.

29. Ryves WJ, Harwood AJ. Lithium inhibits glycogen synthase kinase-3 by competition for magnesium. Biochem Biophys Res Commun 2001;280:720–5.

30. Lee DH, Goldberg AL. Proteasome inhibitors: valuable new tools for cell biologists. Trends Cell Biol 1998;8:397–403.

31. Boon K, Caron HN, van Asperen R, et al. N-myc enhances the expression of a large set of genes functioning in ribosome biogenesis and protein synthesis. EMBO J 2001;20:1383–93.

32. Seo J, Bakay M, Chen YW, et al. Optimizing signal/noise ratios in expression profiling: project-specific algorithm selection and detection *P* value weighting in Affymetrix microarrays. Bioinformatics 2004.

33. Seeger RC, Wada R, Brodeur GM, et al. Expression of N-myc by neuroblastomas with one or multiple copies of the oncogene. Prog Clin Biol Res 1988;271:41–9.

34. Gross N, Balmas Bourloud K, Brognara CB. MYCN-related suppression of functional CD44 expression enhances tumorigenic properties of human neuroblastoma cells. Exp Cell Res 2000;260:396–403.

35. Judware R, Lechner R, Culp LA. Inverse expressions of the N-myc oncogene and β1 integrin in human neuroblastoma: relationships to disease progression in a nude mouse model system. Clin Exp Metastasis 1995;13:123–33.

36. Flickinger KS, Judware R, Lechner R, Carter WG, Culp LA. Integrin expression in human neuroblastoma cells with or without N-myc amplification and in ectopic/orthotopic nude mouse tumors. Exp Cell Res 1994;213:156–63.

37. Liu JJ, Chao JR, Jiang MC, et al. Ras transformation results in an elevated level of cyclin D1 and acceleration of G1 progression in NIH 3T3 cells. Mol Cell Biol 1995;15:3654–63.

38. Diehl JA, Cheng M, Roussel MF, Sherr CJ. Glycogen synthase kinase-3β regulates cyclin D1 proteolysis and subcellular localization. Genes Dev 1998;12:3499–511.

39. Sherr CJ. Cancer cell cycles. Science 1996;274:1672–7.

40. Chen YF, Chiu HH, Wu CH, et al. Retinoblastoma protein (pRB) was significantly phosphorylated through a Ras-to-MAPK pathway in mutant K-ras stably transfected human adrenocortical cells. DNA Cell Biol 2003;22:657–64.

41. Huang E, Ishida S, Pittman J, et al. Gene expression phenotypic models that predict the activity of oncogenic pathways. Nat Genet 2003;34:226–30.

Clinical Cancer Research

Disruption of Cooperation Between Ras and MycN in Human Neuroblastoma Cells Promotes Growth Arrest

Shira Yaari, Jasmine Jacob-Hirsch, Ninette Amariglio, et al.

Clin Cancer Res 2005;11:4321-4330.